Dynamical Climatology

Development of a revised longwave radiation scheme for an atmospheric general circulation model.

by

A.Slingo and R.C.Wilderspin

DCTN 14

December 1984

Meteorological Office (Met. O. 20)
London Road
Bracknell
Berkshire RG12 2SZ

DYNAMICAL CLIMATOLOGY TECHNICAL NOTE NO. 14

DEVELOPMENT OF A REVISED LONGWAVE RADIATION SCHEME FOR AN ATMOSPHERIC GENERAL CIRCULATION MODEL

by

A. Slingo and R.C. Wilderspin

Submitted for publication in the Quarterly Journal of the Royal Meteorological Society.

Met O 20 (Dynamical
Climatolgy Branch)
Meteorological Office
London Road
Bracknell
Berkshire, U.K. RG12 2SZ

December 1984

NOTE: This paper has not been published. Permission to quote from it should be obtained from the Assistant Director of the above Meteorological Office Branch.

SUMMARY

This paper describes the development of a new version of the longwave part of the radiation scheme used in the Meteorological Office 11-Layer Atmospheric General Circulation Model. The work was initiated when comparisons with other radiation schemes revealed systematic errors in the longwave fluxes. A detailed investigation of these errors was carried out by examining the sensitivity of the scheme to many of the details of its formulation. Various improvements were made, notably to the treatment of the temperature-dependence of the Planck function and the water vapour continuum absorption. It is demonstrated that the fluxes are extremely sensitive to the formulation of the continuum absorption and suggested that more observations are needed to refine the values of the absorption coefficients. Special attention was paid to the treatment of carbon dioxide (CO_2) absorption, as the model is being used to continue research on the effect of increasing CO_2 concentrations on climate. A simple scaling of the absorber amounts is applied in order to include the temperature dependence of the CO_2 absorption. It is demonstrated that fluxes from the new version of the scheme and the sensitivity of the fluxes to changing CO_2 concentrations in realistic atmospheres are in excellent agreement with those from more detailed models.

1. INTRODUCTION

One of the most important components of an Atmospheric General Circulation Model (AGCM) is the radiation scheme, which computes both the field of shortwave heating due to the absorption of the incoming solar radiation and the field of longwave cooling from the compensating emission back to space. It is important that such a scheme should not only be numerically fast but also as accurate as possible, especially when the model is to be used for investigating the response of climate to a radiative perturbation, such as that due to increasing carbon dioxide concentrations, and particularly when an interactive ocean surface is employed. It is thus fortunate that the radiation scheme is the only component which may be run independently of the rest of the model and checked against more detailed schemes.

A large number of papers describing new radiation schemes have appeared in the last few years. Until recently, no systematic intercomparison of these schemes had been made in order to understand the differences in the modelled fluxes and to identify systematic errors. Limited comparisons were performed as part of the U.S. carbon dioxide research program (Luther 1983). A much broader international effort known as the Inter-Comparison of Radiation Codes used in Climate Models (ICRCCM) has recently started, the first stage being a detailed comparison of longwave fluxes under cloud-free conditions (Luther et al 1984).

In this paper, comparisons with several other schemes are used to guide the development of a revised version of the longwave part of the radiation scheme in the Meteorological Office 11-Layer AGCM. The work was originally motivated by the need to remove certain systematic errors, which are discussed in section 3. These errors were removed by making changes to the treatment of the Planck function and the spectral resolution (section 4) and of the water vapour continuum absorption (section 5). In addition, a simple parametrization of the temperature dependence of carbon dioxide absorption is presented in section 6 and compared with the more detailed models developed by Kiehl and Ramanathan (1983). The results are not specific to the 11-Layer Model and they address several points which are relevant to a wide range of radiation schemes, particularly in their application to the carbon dioxide/climate problem. The sensitivity of the fluxes to the formulation of the water vapour continuum demonstrates the need for more reliable information on the strength of the absorption and of its wavelength and temperature dependence. The effect of these and other changes on the quality of simulations with the 11-Layer Model will be discussed in a subsequent paper.

2. ORIGINAL VERSION OF THE LONGWAVE RADIATION SCHEME

A description of the 11-Layer Model has not yet appeared in the open literature and so an account of the longwave part of the radiation scheme will be given here. In the original version of the scheme, seven spectral divisions are used to represent the complex wavelength dependence of atmospheric absorption and emission, these being grouped into five distinct intervals as shown in Figure 1. The first interval treats both the

near-infrared vibration/rotation band and the far-infrared rotation band of water vapour. The second and third intervals deal with the overlap between water vapour and the 15 μm band of carbon dioxide (CO_2). The final two intervals cover the contributions in the atmospheric window from weak water vapour lines, the 9.6 μm ozone band and the water vapour continuum absorption. Note that the continuum treatment only partially overlaps the CO_2 band, ending at 700 cm^{-1}.

The equations for the downward and upward longwave fluxes at pressure p are:

$$F^{\downarrow}(p) = B(o).\epsilon(o,p) - \int_{p}^{o} a(p',p) \frac{dB(p')}{dp'} dp' \qquad (1)$$

$$F^{\uparrow}(p) = B(p_s) + \int_{p_s}^{p} a(p',p) \frac{dB(p')}{dp'} dp' \qquad (2)$$

where B(p) is the Planck flux for the temperature of the air at pressure p, B(o) is thus the Planck flux for the top of the atmosphere, which is assumed to be the same as that for the top model level, and $B(p_s)$ is that for the surface. This formulation assumes that the air close to the surface is at the same temperature as the surface itself, which is a reasonable approximation in calculating the fluxes. $\epsilon(o,p)$is the emissivity of the atmosphere from the top down to pressure p and a(p'.p) is the absorptivity from the dummy pressure p' to p. Equations 1 and 2 are essentially the same as equations 2 and 3 of Ramanathan et al (1983), except for slight differences in nomenclature. The equations are solved numerically by a simple trapezoidal rule to calculate fluxes at the layer

boundaries, which are then differenced to give the layer cooling rates. The Planck fluxes are calculated at the 11 atmospheric levels and at the surface and are assumed to vary linearly between these levels. The vertical grid of the model is illustrated by Figure 4 of Slingo (1980).

The emissivity and absorptivity in the above equations are for the entire longwave spectrum and are calculated in a separate subroutine in which the contributions from each spectral band are added:

$$\epsilon(o,p) = \sum_{j=1}^{N} \epsilon_j(o,p) \qquad (3)$$

$$a(p',p) = 1 - \sum_{j=1}^{N} \bar{\tau}_j(p',p) \qquad (4)$$

where ϵ_j and $\bar{\tau}_j$ are the emissivity and transmissivity in the spectral band j and N is the number of bands.

For a band in which water vapour is the only absorber, the emissivity and transmissivity in equations 3 and 4 are simply those for water vapour, calculated for the absorber amounts for the given path by interpolation from look-up tables stored in the program (see appendix). For bands with two or more absorbers the emissivities and transmissivities for each gas are combined by making the usual assumption that the transmissivities may be multiplied together to give the overlapped values. The look-up tables were calculated by applying the version of the Goody random band model described by Hunt and Mattingly (1976) to the spectroscopic data of McClatchey et al (1973). The emissivities and transmissivities are stored

for a temperature of 263 K and the temperature dependence is ignored. The absorber amounts are scaled to take account of the pressure dependence of the line half-widths, by a factor $p^{0.9}$ for water vapour and CO_2 and $p^{0.4}$ for ozone. The continuum treatment is based on the data of Bignell (1970) and depends on the water vapour partial pressure, but the temperature dependence is ignored. The mass mixing ratios of the gases are defined at the model levels and are assumed to be constant within each layer. The mixing ratio of CO_2 is taken to be 4.9×10^{-4} throughout the model, corresponding to 323 parts per million by volume (ppmv).

The relative contribution of each spectral band to the total flux depends on the fraction α_j of the Planck flux in that band at temperature T:

$$\alpha_j = \int_j B(w,T)dw/B(T) \qquad (5)$$

where w is wavenumber and the limits of the integral are the edges of the j^{th} band. Also

$$B(T) = \int_0^{\infty} B(w,T)dw = \sigma T^4 \qquad (6)$$

where σ is the Stefan-Boltzmann constant.

The contributions thus change with increasing temperature as the peak of the Planck function moves to shorter wavelengths. However, in the original version of the scheme this effect was ignored and the α_j were

fixed at their values for 263 K by using emissivities and transmissivities as defined in the appendix. It will be shown later that this is an unnecessarily restrictive assumption which contributes to the errors discussed in the next section.

3. SYSTEMATIC ERRORS IN THE LONGWAVE FLUXES

A survey of observed and calculated longwave fluxes for the cloud-free tropical atmosphere showed that the scheme described in the previous section underestimates the downward longwave fluxes in the lower troposphere by up to about 30 Wm^{-2} (Rowntree, 1981). This is illustrated in Figure 2, which shows upward and downward longwave fluxes for the Tropical profile of McClatchey et al (1971) as given by the 11-Layer Model, the Roach and Slingo (1979) scheme (RS) and a recent version of the Ellingson and Gille (1978) scheme (EG), incorporating minor changes. The EG scheme is a spectrally-detailed model which was shown by them to produce radiance spectra in very good agreement with satellite observations. The fluxes were calculated for the same vertical grid as the profile data, without interpolation, and were kindly provided by Dr R.G. Ellingson. For the other two schemes the data were interpolated; in the case of the 11-Layer Model to the same vertical grid used in the AGCM and for RS to 50 levels, uniformly-spaced in pressure from the surface to the top of the atmosphere.

Figure 2 shows that in the lower troposphere the fluxes from RS are within 5 Wm^{-2} of those from EG, although in the upper troposphere and stratosphere there are larger systematic deviations. Downward fluxes from

the 11-Layer Model are significantly smaller than those from the other schemes in the lower troposphere, the largest difference being over 30 Wm^{-2} at 800 mb. At the surface the difference is about 20 Wm^{-2}, so that the net surface longwave cooling of 60 Wm^{-2} given by the other schemes is over-estimated by about 30 per cent. The first three entries in Table 1 show the fluxes at the top and bottom of the atmosphere from each scheme for all the five standard atmospheres listed by McClatchey et al (1971). The downward fluxes at the surface from RS are larger than those from EG, but the biggest difference is only 6.3 Wm^{-2}, whereas the 11-Layer Model fluxes are from 16.3 Wm^{-2} to 21.6 Wm^{-2} lower than the EG values. The upward fluxes at the top of the atmosphere are much closer, but as shown by Figure 2 the divergence of the upward flux is always much less than that of the downward flux so the better agreement here is not surprising.

The good agreement between RS and EG demonstrates that insufficient spectral resolution is not the reason for the errors in the 11-Layer Model fluxes, as RS has even fewer spectral intervals, as shown on Figure 1. The spectral line data in RS come from the same compilation as the 11-Layer Model and were obtained using the same band model, although in other respects there are many differences between the schemes. It was decided to investigate the errors in the 11-Layer Model fluxes by progressively changing the model to remove the major differences in formulation compared with RS. It must be appreciated that the RS scheme was not treated as an absolute reference but merely as a convenient tool for carrying out the investigation.

Firstly, code was added to the 11-Layer Model to break the fluxes down into the contributions from each spectral band, so that the role of each band could be determined. Secondly, the calculation of the absorber amount in each layer was checked by temporarily changing the pressure and temperature scaling in RS to match that in the 11-Layer Model. This showed that there were no significant differences between the schemes in this calculation.

The following three sections describe the changes to the 11-Layer Model scheme and examine the effect on the fluxes. The results are presented in Tables 1 and 2, the latter showing the vertical profile of the downward fluxes for the Tropical atmosphere. Corresponding tables for the other four atmospheres are not shown because the patterns of the flux differences brought about by the changes are similar, except where discussed in the text.

4. CHANGES TO THE SPECTRAL DATA, PLANCK FUNCTION AND SPECTRAL BANDS

(a) Spectral data

The first change to the model was to re-calculate the emissivity and transmissivity tables using the more recent compilation of spectral line data described by Rothman (1981). The fluxes from this version (2 in Tables 1 and 2) show only small changes compared with the original. Except close to the surface in the Tropical profile, the atmospheric emission is

reduced, so the downward fluxes are lower (by up to 2.4 Wm^{-2} at 375 mb in the Tropical profile, with smaller changes at the surface) and the upward flux at the top of the atmosphere is larger.

(b) Planck function

As described earlier, in the original version of the 11-Layer Model the temperature-dependence of the fraction of the Planck flux in each spectral band was ignored, whereas in RS this is accounted for. To include this effect the look-up tables of emissivity and transmissivity were first normalized as described in the Appendix. Equation 5 was solved numerically for each band using 1 cm^{-1} spectral resolution for 5 K temperature intervals from 180 K to 320 K. The fluxes were then fitted with a second-order polynomial in temperature and the coefficients stored in the program, to allow rapid calculation of the flux in each band. Equations 1 and 2 were altered to calculate the fluxes for each band in turn, which are summed to give the broad-band values. In the Tropical profile the fluxes from this version (3) show an increase by 7.8 Wm^{-2} at 658 mb, decreasing towards the surface. In the colder profiles the level of maximum increase moves to lower levels, so that in the Sub-Arctic Winter profile it is at the surface, where the increase of 9.2 Wm^{-2} removes about half the disagreement with the RS and EG schemes.

The reason for this response is that at 263 K the fraction of the Planck flux in the first spectral band (0-500 and greater than 1200 cm^{-1}) is smaller than at lower temperatures more typical of the upper troposphere, whereas for the atmospheric window bands it is larger. The

importance of the far-infrared rotation band of water vapour, which provides most of the downward long wave flux from the upper troposphere, is thus reduced when the temperature dependence is ignored so that the downward fluxes are too low. The underestimate increases from the top of the atmosphere down to the level where the air temperature is about 263 K and thereafter decreases, so the level of maximum change moves from the mid-troposphere in the warmest profiles to the surface in the Sub-Arctic Winter profile.

(c) Spectral Bands

Further comparisons between the 11-Layer Model and RS were made difficult by the different configurations of the spectral bands, in particular the fact that the 11-Layer Model had a single band covering both the 0-500 and greater than 1200 cm^{-1} regions. It was also felt that dividing the CO_2 band into two at 700 cm^{-1}, close to the centre of the band, might not be justifiable and that the assumption of random overlap between CO_2 and water vapour lines might be questionable in the 500-700 cm^{-1} region, because CO_2 absorption is strongest near 660 cm^{-1} (where the water vapour line absorption is much weaker) and is weak below 600 cm^{-1} (where the water vapour line absorption is stronger) (Rowntree 1981), as for example shown by Figure 1 of Kiehl and Ramanathan (1983). It was therefore decided to change the spectral resolution in these regions to be closer to that of RS, leaving the treatment of the atmospheric window unchanged. Given that RS does not include water vapour continuum absorption outside the window, a proper comparison first required removal of the overlap term 9 from the 11-Layer Model (Figure 1). The effect is shown by

version 4 compared with 2 in Tables 1 and 2. As expected, there is a large response at the surface for the Tropical profile (-11.5 Wm^{-2}) which decreases rapidly with height and is much smaller in the cold profiles. This demonstrates the importance of the continuum term outside the window, which is examined more closely in the next section.

Three major changes to the band configuration were made for version 5. Separate water vapour bands covering 0-560 cm^{-1} (corresponding to RS bands 1 and 2) and 1200 cm^{-1} upwards (roughly equivalent to RS band 5) and a water vapour/CO_2 overlap band covering 560-800 cm^{-1} without a continuum overlap term (corresponding to RS band 3) were included. The effect is to increase the downward fluxes in the lower troposphere, the largest response being at the surface and varying from 5.1 Wm^{-2} to 2.3 Wm^{-2}, with a very small reduction at upper levels. When the temperature dependence of the fraction of the Planck flux in each band is added to produce version 6 there is a slightly larger response compared with that from the version with the original spectral bands (3). The downward flux at the surface in the Sub-Arctic Winter profile is now even closer to that given by RS and EG, but there is still a large discrepancy for the warmer profiles.

The reason for the remaining discrepancy compared with RS for the Tropical profile becomes clear on comparing the fluxes for particular spectral regions. Figure 3 shows a comparison of the fluxes for the four spectral regions where the band limits are now either identical or very similar. For the first two regions (0-560 and 560-800 cm^{-1}) the band limits are identical and the fluxes are close, although downward fluxes from the 11-Layer Model are a few Wm^{-2} lower than those from RS throughout

the troposphere in both regions. This might be due to ignoring the temperature dependence of the spectral line data but it is dangerous to rely on such small differences as the analytic fits to the transmissivities employed in RS are not of high accuracy. For the near-infrared band of water vapour, the 11-Layer Model band is narrower than that of RS and thus is bound to contain less flux, as shown by the difference between the upward fluxes from the surface. Taking this into account it is difficult to find evidence for more than a few Wm^{-2} underestimate by the 11-Layer Model in this region. In the window, the 11-Layer Model uses a wider spectral range as shown by the larger upward fluxes. To be consistent with RS the downward fluxes should also be larger but in fact they are about 10 Wm^{-2} lower. Clearly, the remaining discrepancy is mainly due to differences in the treatment of the water vapour continuum, which provides most of the downward flux in the window in clear tropical atmospheres. This fact is graphically illustrated by the filled dots on Figure 3, which show the downward window fluxes from version 6 when the continuum term is removed. In the following section, a revised treatment of the continuum in the window and at longer wavelengths is described.

5. CHANGES TO THE TREATMENT OF THE WATER VAPOUR CONTINUUM

(a) Window continuum

The existing continuum treatment was first replaced by that of RS (section 3b), which follows Bignell (1970) and is equivalent to that used by EG. There are two contributions to the continuum absorption; a "foreign-broadened" coefficient k_1, arising from broadening of water vapour

lines by collisions with other gases, and an "e-type" coefficient k_2 which is usually attributed to the dimer molecule $(H_2O)_2$. The values of k_1 and k_2 and their temperature-dependence were taken from RS. The effect of this change is shown by the fluxes from version 7 compared with version 6. There is a substantial increase in the downward fluxes (as also shown by the open circles on Figure 3), the surface value increasing by 19 Wm^{-2} for the Tropical profile and by 2.7 Wm^{-2} for the Sub-Arctic Winter profile. The downward flux at the surface is now within a few Wm^{-2} of that from both RS and EG. However, this apparent agreement is misleading as there are still differences between the schemes. For example, RS ignores the effect of local water vapour lines in the window while EG includes a continuum term not only in the window but across the CO_2 band to end at 400 cm^{-1}. In this section the effect of a revised continuum treatment for the 11-Layer Model which also covers this range will be examined.

Two aspects of the continuum treatment described by RS were changed. Firstly, there seems to be little evidence to support the weak $T^{1.5}$ temperature dependence for the foreign broadened coefficient k_1, so this was removed. Secondly, the temperature dependence for the e-type coefficient k_2 was changed to that described by Roberts et al (1976), using their best estimate of T_o = 1800 K for the temperature dependence parameter;

$$k_2(T) = k_2(296K) \exp[T_o/T - T_o/296] \qquad (7)$$

At the new reference temperature of 296 K the values of the continuum coefficients were taken to be $k_1 = 0.05\ g^{-1}\ cm^2\ atm^{-1}$ and $k_2 = 10\ g^{-1}\ cm^2\ atm^{-1}$ for both bands 4 and 5 in the window. The ratio of k_1 to k_2 is thus 0.005, which was also used by EG. The effect of these changes (Version 8) is to weaken the window continuum compared with RS, the largest flux change being $-8.3\ Wm^{-2}$ at the surface for the Mid-Latitude Summer profile.

(b) 15 μm continuum

In section 4(c) it was shown that removal of the continuum term overlapping CO_2 in the 700–800 cm^{-1} region reduced the surface downward flux by up to 11.5 Wm^{-2}. Such a term thus makes an important contribution in this region and when it is extended to cover the entire 15 μm band it significantly reduces the sensitivity of the net surface flux in moist atmospheres to increased CO_2 concentrations (Kiehl and Ramanathan 1982). Both Bignell (1970) and Roberts et al (1976) show that the e-type continuum is stronger at these wavelengths than in the 10 μm window. From Bignell's data the mean value of k_2 in the 560–800 cm^{-1} interval was taken to be $30\ g^{-1}\ cm^2\ atm^{-1}$ with the same temperature dependence as in the window and with $k_1/k_2 = 0.005$. The 15 μm continuum was included in Version 9 as an overlap term in addition to the terms from water vapour and CO_2 lines. The effect is to increase the downward fluxes by up to 13 Wm^{-2} for the Tropical profile at the surface and by smaller amounts in the other profiles. The effect on the sensitivity to doubled CO_2 concentrations will be examined in section 6.

(c) 20 μm continuum

Bignell (1970) and Roberts et al (1976) show that the strength of the continuum absorption continues to increase beyond the 15 μm band to at least 400 cm^{-1} (25 μm wavelength). There seems little point in including a continuum term at longer wavelengths because the strong absorption by the far-infrared rotation band of water vapour ensures that fluxes are already close to the Planck values in this spectral region in the lower troposphere. However, there is a weak window at about 20 μm where the continuum might be important. The 0-560 cm^{-1} band was therefore divided into two, as in RS, and the continuum included as an overlap term with water vapour lines in the 400-560 cm^{-1} region. The effect of dividing the band before adding the continuum term is given by comparing versions 10 and 9 in the tables. The effect at the surface is small but it increases with height to a maximum of 1.8 Wm^{-2} at 375 mb in the Tropical profile and 2.4 Wm^{-2} at 517 mb in the Sub-Arctic Winter profile. These are the levels where the flux divergence in the rotation band, and hence the cooling rate, is greatest and it is therefore not surprising to find a sensitivity when improved spectral resolution is incorporated.

The mean value of k_2 in the 400-560 cm^{-1} band was taken from Bignell's (1970) data to be 70 g^{-1} cm^2 atm^{-1} with the same temperature dependence and ratio of k_1 to k_2 as in the window and at 15 μm. The final configuration of the spectral bands and overlaps used in this version (11) is shown on Figure 1. The response to this term is significant and justifies its inclusion. In the Tropical profile the downward flux increases by 7.1 Wm^{-2} at 800 mb and by 3.5 Wm^{-2} at the surface. In the other profiles

the maximum increase moves towards the surface so that in the Sub-Arctic Summer profile the surface flux increases by more (5.8 Wm^{-2}) than in the Tropical profile, while in the Sub-Arctic Winter profile the maximum is at the surface itself but smaller in magnitude (3.4 Wm^{-2}).

(d) Discussion

It is well known that the water vapour continuum term makes a substantial contribution to the net longwave flux at the surface in warm, moist atmospheres. For example, if all the continuum terms are removed from Version 11 the surface downward flux in the Tropical profile drops by 87.2 Wm^{-2}, thus enhancing the surface longwave cooling by over two and a half times. This emphasizes the accuracy which is required in calculating this term, although there is still no clear consensus on the magnitude of the absorption coefficients and their variation over wide ranges of temperature. For example, the somewhat arbitrary ratio $k_1/k_2 = 0.005$ has been used here, whereas Bignell (1970, Figure 8) shows evidence that k_1/k_2 is much larger than this at about 20 μm, although Roberts et al (1976) suggest that it is much smaller and that k_1 should be ignored at all wavelengths. The effect of removing k_1 altogether in all the continuum bands but retaining k_2 is shown by comparing versions 12 and 11. In the Tropical profile the largest response is at 912 mb (-9.7 Wm^{-2}) and the surface flux drops by almost as much (9.3 Wm^{-2}). Most of the change at the surface (8.7 Wm^{-2}) is due to the window bands (800-1200 cm^{-1}) but at higher levels the 15 μm and 20 μm contributions are as important. In the other profiles the maximum response is at the surface, varying from -10.5 Wm^{-2} for the Mid-Latitude Summer to -4.0 Wm^{-2} in the Sub-Arctic Winter profiles.

These changes are of similar magnitude to those resulting from the inclusion of the 15 μm continuum and underline the need for more reliable information on the magnitude of this term as well as of k_2.

Version 11 of the 11-Layer Model longwave scheme was now rationalised to remove redundant code and optimised for efficient execution in the full model on the Cyber 205 computer. It was found convenient to alter the subroutine which calculates ϵ and a to calculate directly the B(o). $\epsilon(o,p)$ and integral terms in equations 1 and 2, thus calculating the flux contributions from each band and each layer. To implement this the look-up tables of ϵ_j and τ_j were normalised to unity (see Appendix). The fit to the fraction of the Planck flux in each band was replaced by one to calculate the fluxes directly (by removing the denominator from equation 5), which required a third order as opposed to a second order polynomial in temperature. The difference between the fluxes from this "intermediate" version (13) and version 11 are very small, the largest difference being $-0.4\ Wm^{-2}$ for the upward flux at the top of the atmosphere from the Tropical profile.

6. CHANGES TO THE TREATMENT OF CARBON DIOXIDE

One of the most important applications of the 11-Layer Model is to continue work on the effect of increasing carbon dioxide (CO_2) concentrations on climate (Mitchell 1983). It is obviously important that the radiative effects of CO_2 applied to the model should be as accurate as possible. Results from the model are here compared with the work of Kiehl and Ramanathan (1983) (hereafter KR), who carried out a detailed comparison

of fluxes from a new Wide Band scheme, designed for fast computation in climate models, with those from Goody and Malkmus Narrow Band Models. They showed that as regards accuracy there was little to choose between the three schemes, although the best agreement with measured absorptances was obtained with the Malkmus and Wide Band models..

In the simplest comparison, fluxes for isothermal atmospheres at 200 K and 300 K in which CO_2 is the only radiatively-active gas were calculated for CO_2 concentrations of 320 and 640 ppmv. Results for the downward flux at the surface for the models studied by KR and versions of the present scheme are shown in Table 3. At 200 K, the fluxes and sensitivity to changing CO_2 from the original version of the present scheme are over-estimated compared with KR, whereas at 300 K there is good agreement. The intermediate version (13 in Tables 1 and 2) shows improved fluxes and sensitivity at 200 K, but at 300 K both are too low. The pattern of the differences between this version and KR suggested that they might be reduced by including the temperature dependence of the CO_2 absorption. This has long been known to be significant, with emissivities which increase steadily with increasing temperature (e.g. Liou 1980, Figure 4.8), such that using values for 263 K at all temperatures (as in this version) would be expected to over-estimate emissivities at lower temperatures and under-estimate them at higher temperatures. Figure 4 shows curves of the normalized emissivity of CO_2 in the 560-800 cm^{-1} band as a function of the absorber amount u for various temperatures T, as given by the band model (at 40 cm^{-1} resolution). The shape of the curves, which diverge steadily with increasing u, suggested that a reasonable approximation to the emissivity at any temperature could be obtained by using the curve for

263 K as before, but in addition scaling the absorber amounts with a temperature-dependent factor which is itself a function of absorber amount. After some experimentation, it was found that the following scaling of the absorber amount in each layer, Δu, was adequate;

$$\Delta u_{SCALED} = \Delta u . (T/263)^{POWER} \quad (8)$$

where

$$POWER = 8.5 + 2 \log_{10}(\Delta u) \quad (9)$$

where T is the layer temperature. At small Δu, POWER is forced to be zero rather than become negative. The dots on Figure 4 show the effective emissivities at the layer boundaries for a CO_2 concentration of 320 ppmv, obtained by using this scaling for temperatures of 203 and 323 K, which demonstrates the excellent fit to the data. Note that the dependence of the scaling on the absorber amount results in a shift of the effective emissivity curves as the CO_2 concentration is increased, but the effect on the sensitivity of the scheme to changing CO_2 amounts is very small.

This scaling represents the final change to create the New version of the radiation scheme (14). Table 3 shows that the fluxes and sensitivity to doubled CO_2 for this version are in excellent agreement with KR at 200 K. At 300 K the fluxes are also in good agreement although the sensitivity to doubled CO_2 is still low. Fluxes using this version are also entered in Tables 1 and 2. As expected, the scaling reduces the downward fluxes at upper levels and increases the outgoing longwave flux, with smaller changes at the surface.

Although results for isothermal atmospheres are useful in studying the temperature dependence, it is also important to check the CO_2 fluxes for more realistic atmospheres. Table 4 shows a comparison of the sensitivity to doubling CO_2 of the original and new versions of the scheme with that of the schemes used by KR, for three atmospheres in which CO_2 is the only absorber. In addition, results for the Tropical profile when the overlap of the CO_2 band by water vapour line and continuum absorption are also included are shown in brackets. The values for the Wide Band model are different from those given by KR as they come from a more recent version (Kiehl, in preparation). This employs a new vertical finite difference scheme to determine the mean temperature used in the calculation of the CO_2 absorption, leading to fluxes which are in better agreement with the narrow band model results when CO_2 is the only absorber. There is also a revised formulation of the mean water vapour absorption across the wide band. Neither change affects the results shown in Table 3.

The change in the downward flux at the surface for the New version of the scheme is lower than in KR for all three atmospheres when CO_2 is the only absorber, while the original version gives values which are closer to KR. However, this disparity disappears when the overlapping by water vapour is included in the tropical profile, when all the models predict a much smaller change because the enhanced CO_2 flux is absorbed by water vapour in the lower troposphere before it can reach the surface. This effect is weakest in the original version of the 11-Layer Model scheme because the continuum term does not cover the entire CO_2 band but only the

700-800 cm^{-1} region (see Figure 1). It is much stronger in the New version of the scheme and the essential result that the change in the surface flux is reduced to a low value agrees well with KR.

The response of the climate system to changing CO_2 concentrations is controlled more by the change in the net upward flux at the tropopause than by that at the surface (e.g. Ramanathan 1981). Table 4 shows that for this parameter the original version of the 11-Layer Model scheme gives values for the two warm profiles which are larger than those obtained by KR, whereas the values from the new version are much closer. All five schemes show good agreement for the winter profile. The effect of including the water vapour absorption in the Tropical profile is to reduce the flux change to on average -5.35 Wm^{-2} for the three schemes considered by KR. The value from the original version of the 11-Layer Model scheme is higher (-6.15 Wm^{-2}), but that from the new version (-5.26 Wm^{-2}) is again closer to KR. It is thus reasonable to conclude that the new version shows a sensitivity to changing CO_2 concentrations in realistic atmospheres which compares very favourably with the schemes developed by KR.

7. DISCUSSION

Figure 2 shows that the changes described in the previous sections to create the new version of the 11-Layer Model longwave radiation scheme have removed the systematic errors in the fluxes from the original version. Compared with the EG scheme, there is still evidence that the downward fluxes in the middle troposphere are too low, but by at most 10 Wm^{-2} compared with 30 Wm^{-2} previously. At the surface, the new scheme gives

downward fluxes which are up to about 10 Wm^{-2} larger than EG, but it has been shown that the surface flux is extremely sensitive to the formulation of the water vapour continuum absorption. Clearly, more observations are needed to refine the values of the continuum absorption coefficients and in particular to establish the validity of the temperature-dependence assumed for the e-type component over a wider range of temperature and wavenumber and to confirm or disprove the existence of the foreign-broadened component. It is recognised that it is easy to make such recommendations when the authors do not have to make the observations, but this is clearly still an uncertain area.

This study has demonstrated the value of detailed comparisons between radiation schemes to establish the reasons for differences in the predicted fluxes. While some modellers may wish to pursue even small flux differences to provide a complete explanation, the authors' experience is that this is a time-consuming process. There comes a point in developing an AGCM where that time is best spent on other more uncertain areas of the model. The AGCM modeller thus needs to know how the flux differences of the magnitude studied here affect the quality of simulations with the model, in order to assess the impact and importance of flux errors on the model's climate. The effect of these and other radiation scheme changes on the climate of the 11-Layer AGCM will therefore be described in a subsequent paper.

ACKNOWLEDGEMENTS

J.T. Kiehl, V. Ramanathan and R.G. Ellingson kindly provided fluxes from their radiation schemes which proved to be invaluable in the work reported here. D.R. Pick is thanked for making available the data tape of spectral line data and a program to read it. D.E. Chapman provided useful information on the random band model. We acknowledge the constructive criticism of the manuscript by P.R. Rowntree and J.M. Slingo.

APPENDIX: DERIVATION OF THE EMISSIVITY AND TRANSMISSIVITY TABLES FOR EACH GAS

The data source for the original version of the longwave scheme was the compilation by McClatchey et al (1973) of, among other quantities, the line strength s_i and line width α_i for over 100,000 lines of various gases from a wavelength of less than 1 μm to the far infrared. A computer program was used to extract the data for each gas in each spectral interval. The line strengths and widths, listed on the tape for 296 K, were converted to values at 20 K intervals from 180 to 320 K using equations 4-7 of Hunt and Mattingly (1976). The quantities $\Sigma\, s_i$ and $\Sigma\, \sqrt{s_i \alpha_i}$ were then calculated in sub-intervals (typically 50 cm^{-1}) within which the Planck function may be taken to be constant. In the band model program, the slab transmission τ in each sub-interval at 30 K intervals from 203 to 323 K and at a pressure of 1000 mb was calculated for a range of absorber amounts u from 10^{-10} to 10^{2} g cm^{-2} in half-decade intervals using equations 1-3 of Hunt and Mattingly (1976). The integration over zenith angle was performed by Gaussian quadrature to avoid the need for a diffusivity factor in the radiation scheme. These tranmissions were weighted with the Planck function to derive the mean transmissivity $\bar{\tau}$ and emissivity ϵ in spectral band j for gas k;

$$\bar{\tau}_{j,k}(u,T) = \int_j \tau_k(\omega,u,T) \cdot \frac{dB(\omega,T)}{dT}\, d\omega \Big/ \int_0^\infty \frac{dB(\omega,T)}{dT}\, d\omega \qquad (A.1)$$

$$\epsilon_{j,k}(u,T) = \int_j (1-\tau_k(\omega,u,T)).B(\omega,T).d\omega \Big/ \int_0^\infty B(\omega,T)d\omega \qquad (A.2)$$

Note that $$\int_0^{\infty} \frac{dB(\omega,T)}{dT}\, d\omega = \frac{dB(T)}{dT} = 4\sigma T^3 \qquad (A.3)$$

The values of emissivity and transmissivity are stored in the radiation scheme as look-up tables as a function of absorber amount for each of the terms shown for H_2O, CO_2 and O_3 in Figure 1, for T = 263 K only. The temperature dependence of the spectral line data and of the fraction α_j of the Planck flux in each spectral band (see section 2) are thus ignored. Note that the wavenumber limits on integrals A.1 and A.2 ensure that the maximum value which $\epsilon_{j,k}(u,T)$ may attain is equal to α_j (equation 5), so that the emissivities and transmissivities may be summed by equations 3 and 4 to produce the broad-band values.

In the new version of the scheme, the emissivities and transmissivities were normalized so that the maximum value obtainable was unity, by changing the limits on the integrals in the denominators of equations A.1 and A.2 to match those of the integrals in the numerators. This then enabled the temperature-dependence of the α_j to be included, as described in section 4b.

REFERENCES

Bignell K.J. 1970 The water vapour infra-red continuum. Quart. J.R. Met. Soc., 96, 390-403.

Ellingson R.G. and Gille J.C. 1978 An infrared radiative transfer model. Part 1: Model description and comparison of observations with calculations. J.Atmos. Sci., 35, 523-545.

Hunt G.E. and Mattingly S.R. 1976 Infrared radiative transfer in planetary atmospheres - I. Effects of computational and spectroscopic economies on thermal heating/cooling rates. J.Quant. Spectrosc. Radiat. Transfer, 16. 505-520.

Kiehl J.T. and Ramanathan V. 1982 Radiative heating due to increased CO_2: The role of H_2O continuum absorption in the 12-18 μm region. J.Atmos. Sci., 39, 2923-2926.

Kiehl J.T. and Ramanathan V. 1983 CO_2 radiative parametrization used in climate models: Comparison with narrow band models and with laboratory data. J.Geophys. Res., 88, 5191-5202.

Liou K. -N. 1980 An introduction to atmospheric radiation. International Geophysics Series Volume 26, Academic Press.

Luther F.M. 1983 Radiative effects of a CO_2 increase: Results of a model comparison. Proceedings: Carbon Dioxide Research Conference: Carbon Dioxide, Science and Concensus. CONF-820970, p.III. 177-193. U.S. Dept. of Energy, Washington, D.C. 20545.

Luther F.M. and others 1984 Inter-Comparison of Radiation Codes used in Climate Models (ICRCCM). In preparation.

McClatchey R.S., Fenn R.W., Selby J.E.A., Volz F.E. and Garing J.S. 1971 Optical properties of the atmosphere. AFCRL-71-0279, Air Force Cambridge Research Laboratories, Bedford, Mass. USA.

McClatchey R.S., Benedict W.S., Clough S.A., Burch D.E., Calfee R.F., Fox K., Garing J.S. and Rothman L.S. 1973 AFCRL atmospheric absorption line parameters compilation. AFCRL-TR-73-0096, Air Force Cambridge Research Laboratories, Bedford, Mass., USA.

Mitchell J.F.B. 1983 The seasonal response of a general circulation model to changes in CO_2 and sea temperatures. Quart. J.R. Met. Soc., 109, 113-152.

Ramanathan V. 1981 The role of ocean-atmosphere interactions in the CO_2 climate problem. J.Atmos. Sci., 38, 918-930.

Ramanathan V., Pitcher E.J., Malone R.C. and Blackmon M.L. 1983 The response of a spectral general circulation model to refinements in radiative processes. J.Atmos. Sci., 40, 605-630.

Roach W.T. and Slingo A. 1979 A high resolution infrared radiative transfer scheme to study the interaction of radiation with cloud. Quart. J.R. Met. Soc., 105, 603-614.

Roberts R.E., Selby J.E.A. and Biberman L.M. 1976 Infrared continuum absorption by atmospheric water vapour in the 8-12 μm window. Applied Optics, 15, 2085-2090.

Rothman L.S. 1981 AFGL atmospheric absorption line parameters compilation: 1980 version. Applied Optics, 20, 791-795.

Rowntree P.R. 1981 A survey of observed and calculated longwave fluxes for the cloud-free tropical atmosphere. Met O 20 Technical Note No. II/174, (Available from the National Meteorological Library, Meteorological Office, Bracknell).

Slingo J.M. 1980 A cloud parametrization scheme derived from GATE data for use with a numerical model. Quart. J.R. Met. Soc., 106, 747-770.

TABLE 1 Downward longwave flux at the surface and upward flux at the top of the atmosphere (Wm^{-2}) for the Ellingson and Gille (1978) and Roach and Slingo (1979) schemes and various versions of the 11-Layer Model scheme, for all 5 McClatchey et al (1971) profiles.

VERSION	NOTES	DOWNWARD FLUX AT SURFACE					UPWARD FLUX AT TOP OF ATMOSPHERE				
		TROP.	M.L.S.	S.A.S.	M.L.W.	S.A.W.	TROP.	M.L.S.	S.A.S.	M.L.W.	S.A.W.
-	Ellingson and Gille (1978) scheme	396.7	347.0	296.3	217.2	166.3	293.9	285.2	267.1	233.7	200.6
-	Roach and Slingo (1979) scheme	402.2	353.3	299.9	219.5	169.0	288.6	283.6	267.8	232.8	199.8
1	11-Layer Model: Original version	379.8	328.0	274.7	195.8	150.0	297.3	285.4	268.9	232.2	199.3
2	= 1 but new spectral data	379.9	328.0	274.6	195.4	149.4	299.3	287.2	270.3	233.6	200.5
	Effect of " " "	0.1	0	-0.1	-0.4	-0.6	2.0	1.8	1.4	1.4	1.2
3	= 2 plus Planck function temperature dependence	382.8	332.0	279.6	203.9	158.6	298.2	286.5	269.6	232.3	199.0
	Effect of " " " "	2.9	4.0	5.0	8.5	9.2	-1.1	-0.7	-0.7	-1.3	-1.5
4	= 2 with no continuum term 9	368.4	319.0	268.7	193.6	148.8	301.0	288.2	271.1	233.8	200.5
	Effect of " " " "	-11.5	-9.0	-5.9	-1.8	-0.6	1.7	1.0	0.8	0.2	0
5	= 4 but new spectral bands	373.5	323.7	272.9	196.7	151.1	299.2	286.7	269.7	233.1	200.3
	Effect of " " "	5.1	4.7	4.2	3.1	2.3	-1.8	-1.5	-1.4	-0.7	-0.2
6	= 5 plus Planck function temperature dependence	377.3	328.9	279.3	207.9	163.1	298.8	286.3	269.0	231.1	198.0
	Effect of " " " "	3.8	5.2	6.4	11.2	12.0	-0.4	-0.4	-0.7	-2.0	-2.3
7	= 6 but RS window continuum	396.3	347.4	295.0	214.7	165.8	293.4	282.8	265.8	230.3	197.9
	Effect of " " "	19.0	18.5	15.7	6.8	2.7	-5.4	-3.5	-3.2	-0.8	-0.1
8	= 7 but revised window continuum	389.1	339.1	288.2	211.8	164.7	295.5	284.4	267.0	230.6	198.0
	Effect of " " "	-7.2	-8.3	-6.8	-2.9	-1.1	2.1	1.6	1.2	0.3	0.1

TABLE 1 (Contd)

9	= 8 plus 15 μm continuum	402.1	350.9	297.6	215.6	166.1	293.2	282.7	265.6	230.3	197.9
	Effect of " "	13.0	11.8	9.4	3.8	1.4	-2.3	-1.7	-1.4	-0.3	-0.1
10	= 9 but additional 20 μm band	402.1	351.0	297.7	216.1	167.1	293.5	283.0	265.8	230.4	197.8
	Effect of " " "	0	0.1	0.1	0.5	1.0	0.3	0.3	0.2	0.1	-0.1
11	= 10 plus 20 μm continuum	405.6	355.7	303.5	221.5	170.5	291.9	281.6	264.4	229.7	197.6
	Effect of " "	3.5	4.7	5.8	5.4	3.4	-1.6	-1.4	-1.4	-0.7	-0.2
12	= 11 but no k_1 continuum term	396.3	345.2	293.8	214.8	166.5	295.2	284.2	266.8	230.7	197.9
	Effect of " " " "	-9.3	-10.5	-9.7	-6.7	-4.0	3.3	2.6	2.4	1.0	0.3
13	= 11 with minor changes (see text)	405.7	355.8	303.4	221.3	170.2	291.5	281.3	264.2	229.6	197.6
	Effect of " "	0.1	0.1	-0.1	-0.2	-0.3	-0.4	-0.3	-0.2	-0.1	0
14	= 13 plus CO_2 temperature dependence	405.9	356.1	303.8	221.3	169.3	294.9	283.6	266.1	232.1	199.9
	Effect of " " "	0.2	0.3	0.4	0	-0.9	3.4	2.3	1.9	2.5	2.3

KEY: TROP. (Tropical), M.L.S. (Mid-Latitude Summer), S.A.S. (Sub-Arctic Summer), M.L.W. (Mid-Latitude Winter) and S.A.W. (Sub-Arctic Winter).

TABLE 2 Downward longwave fluxes (Wm^{-2}) as a function of pressure for the various versions of the 11-Layer Model scheme, for the McClatchey et al (1971) Tropical profile. Interpolated values from the Ellingson and Gille (1978) and Roach and Slingo (1979) schemes are also shown.

		PRESSURE (mb)										
VERSION	NOTES	1013	988	912	800	658	517	375	274	198	127	61
–	Ellingson and Gille (1978) scheme	396.7	383.3	342.4	283.5	216.3	152.0	89.9	46.0	22.8	13.4	10.8
–	Roach and Slingo (1979) scheme	402.2	388.8	346.0	283.4	215.3	156.6	96.5	53.0	28.4	18.3	15.7
1	Original Version	379.8	361.6	313.8	248.9	185.8	133.4	82.6	43.5	24.5	17.3	15.1
2	= 1 but new spectral data	379.9	361.7	313.8	248.4	184.4	131.4	80.2	41.4	23.1	16.2	14.1
	Effect of " " "	0.1	0.1	0	-0.5	-1.4	-2.0	-2.4	-2.1	-1.4	-1.1	-1.0
3	= 2 plus Planck function temperature dependence	382.8	365.1	318.7	255.6	192.2	138.5	85.3	43.6	23.3	15.8	14.4
	Effect of " " " "	2.9	3.4	4.9	7.2	7.8	7.1	5.1	2.2	0.2	-0.4	0.3
4	= 2 with no continuum term 9	368.4	350.7	304.9	244.0	183.4	131.2	80.2	41.4	23.1	16.2	14.1
	Effect of " " " "	-11.5	-11.0	-8.9	-4.4	-1.0	-0.2	0	0	0	0	0
5	= 4 but new spectral bands	373.5	355.7	309.6	248.2	186.3	132.6	80.3	41.2	22.8	16.1	14.0
	Effect of " " "	5.1	5.0	4.7	4.2	2.9	1.4	0.1	-0.2	-0.3	-0.1	-0.1
6	= 5 plus Planck function temperature dependence	377.3	360.2	316.0	257.3	196.4	141.8	87.0	43.8	23.0	15.7	14.2
	Effect of " " " "	3.8	4.5	6.4	9.1	10.1	9.2	6.7	2.6	0.2	-0.4	0.2
7	= 6 but RS window continuum	396.3	380.0	334.4	269.5	199.8	142.4	87.0	43.8	23.0	15.7	14.2
	Effect of " " "	19.0	19.8	18.4	12.2	3.4	0.6	0	0	0	0	0
8	= 7 but revised window continuum	389.1	372.4	326.8	264.4	198.4	142.1	87.0	43.8	23.0	15.7	14.2
	Effect of " " "	-7.2	-7.6	-7.6	-5.1	-1.4	-0.3	0	0	0	0	0
9	= 8 plus 15 μm continuum	402.1	385.4	339.5	272.8	200.9	142.7	87.1	43.8	23.0	15.7	14.2
	Effect of " "	13.0	13.0	12.7	8.4	2.5	0.6	0.1	0	0	0	0

TABLE 2 (Contd)

10	= 9 but additional 20 μm band	402.1	385.5	339.7	273.1	201.6	144.0	88.9	45.1	23.6	16.1	14.5
	Effect of " " "	0	0.1	0.2	0.3	0.7	1.3	1.8	1.3	0.6	0.4	0.3
11	= 10 plus 20 μm continuum	405.6	389.3	345.1	280.2	206.0	145.5	89.1	45.1	23.6	16.1	14.5
	Effect of " "	3.5	3.8	5.4	7.1	4.4	1.5	0.2	0	0	0	0
12	= 11 but no k_1 continuum term	396.3	379.7	335.4	271.7	201.5	144.0	88.9	45.1	23.6	16.1	14.5
	Effect of " " " "	-9.3	-9.6	-9.7	-8.5	-4.5	-1.5	-0.2	0	0	0	0
13	= 11 with minor changes (see text)	405.7	389.4	345.2	280.2	206.0	145.4	89.0	45.1	23.7	16.1	14.5
	Effect of " "	0.1	0.1	0.1	0	0	-0.1	-0.1	0	0.1	0	0
14	= 13 plus CO_2 temperature dependence	405.9	389.6	345.5	280.9	206.1	144.0	86.2	42.0	21.0	14.4	13.3
	Effect of " " "	0.2	0.2	0.3	0.7	0.1	-1.4	-2.8	-3.1	-2.7	-1.7	-1.2

TABLE 3 Downward longwave fluxes (Wm^{-2}) at the surface due to CO_2 for isothermal atmospheres at 200 K and 300 K for various models.

CASE	KIEHL & RAMANATHAN (1983)			11-LAYER MODEL		
	GOODY	MALKMUS	WIDE BAND	ORIGINAL Version 1	INTER-MEDIATE Version 13	NEW Version 14
T = 200 K						
CO_2 = 320 ppmv	13.3	13.2	13.7	18.37	16.43	13.53
CO_2 = 640 ppmv	14.3	14.3	14.8	19.77	17.52	14.65
640-320	1.03	1.09	1.14	1.40	1.09	1.12
T = 300 K						
CO_2 = 320 ppmv	90	90	89	92.98	85.32	91.33
CO_2 = 640 ppmv	97	97	96	100.07	91.02	97.12
640-320	6.98	6.96	7.10	7.09	5.70	5.79

TABLE 4 Comparison of the change in longwave fluxes (Wm^{-2}) due to doubled CO_2 from the models used by Kiehl and Ramanathan (1983) with the Original and New versions of the 11-Layer Model scheme, for three atmospheres in which CO_2 is the only absorber. The fluxes from the Wide Band model differ from those given by Kiehl and Ramanathan as they come from a more recent version. See text for details. The fluxes obtained for the Tropical profile when the overlap by water vapour line and continuum absorption are added are shown in brackets. $\Delta F^{\downarrow}(S)$ is the change in downward flux at the surface and $\Delta F^{\uparrow}_{NET}(T)$ is the change in the net upward flux at the tropopause.

PROFILE	FLUX	KIEHL & RAMANATHAN (1983)			11-LAYER MODEL	
		GOODY	MALKMUS	WIDE BAND	ORIGINAL Version 1	NEW Version 14
Tropical	$\Delta F^{\downarrow}(S)$	6.80 (0.40)	6.85 (0.40)	7.00 (0.10)	6.69 (1.17)	6.01 (0.21)
	$\Delta F^{\uparrow}_{NET}(T)$	-6.43 (-5.33)	-6.40 (-5.38)	-6.74 (-5.33)	-7.42 (-6.15)	-6.51 (-5.26)
Mid-Latitude Summer	$\Delta F^{\downarrow}(S)$	6.37	6.42	6.55	6.19	5.56
	$\Delta F^{\uparrow}_{NET}(T)$	-6.09	-6.15	-6.35	-6.56	-6.05
Sub-Arctic Winter	$\Delta F^{\downarrow}(S)$	3.79	3.86	3.93	3.65	3.45
	$\Delta F^{\uparrow}_{NET}(T)$	-3.63	-3.72	-3.69	-3.67	-3.72

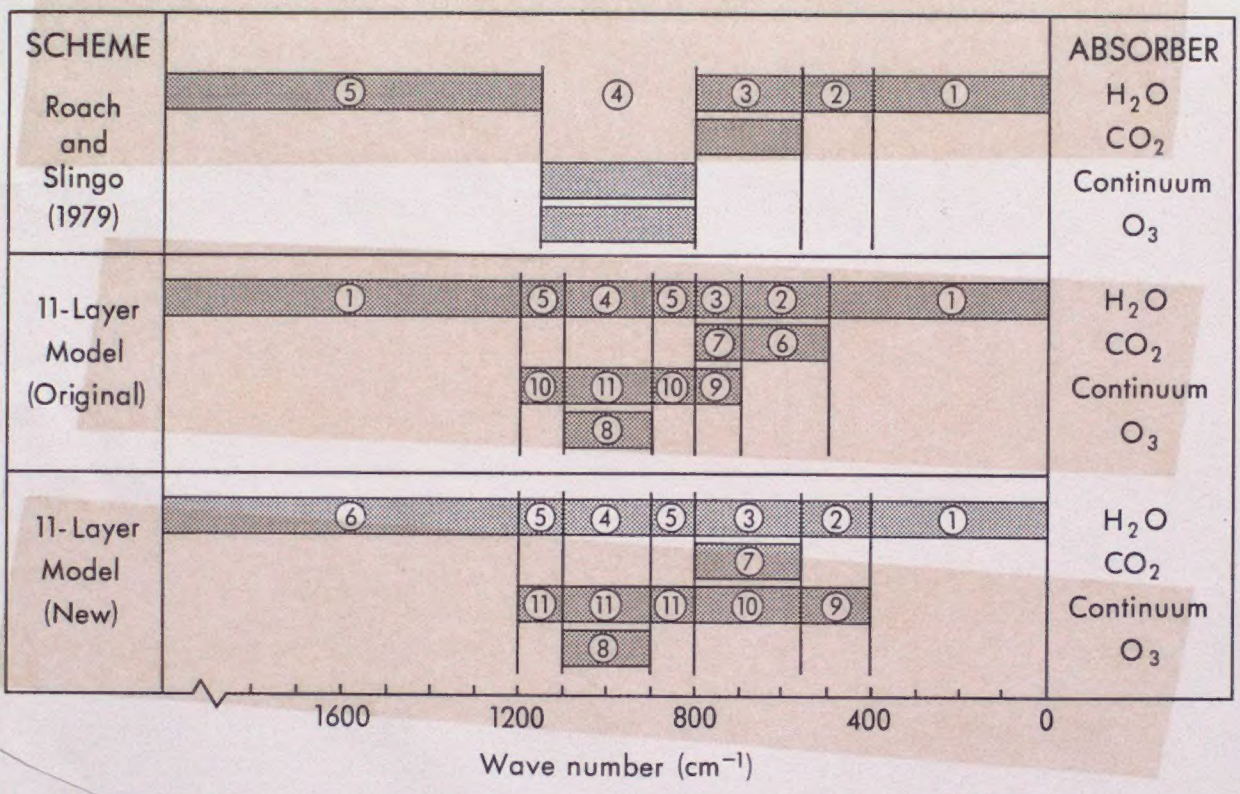

Figure 1 Band limits and absorbers taken into account in the Roach and Slingo (1979) longwave radiation scheme and the original and new versions of the 11-Layer Model scheme. The numbers identify the spectral bands of the former scheme and the separate contributions to the total flux from each absorber for the latter.

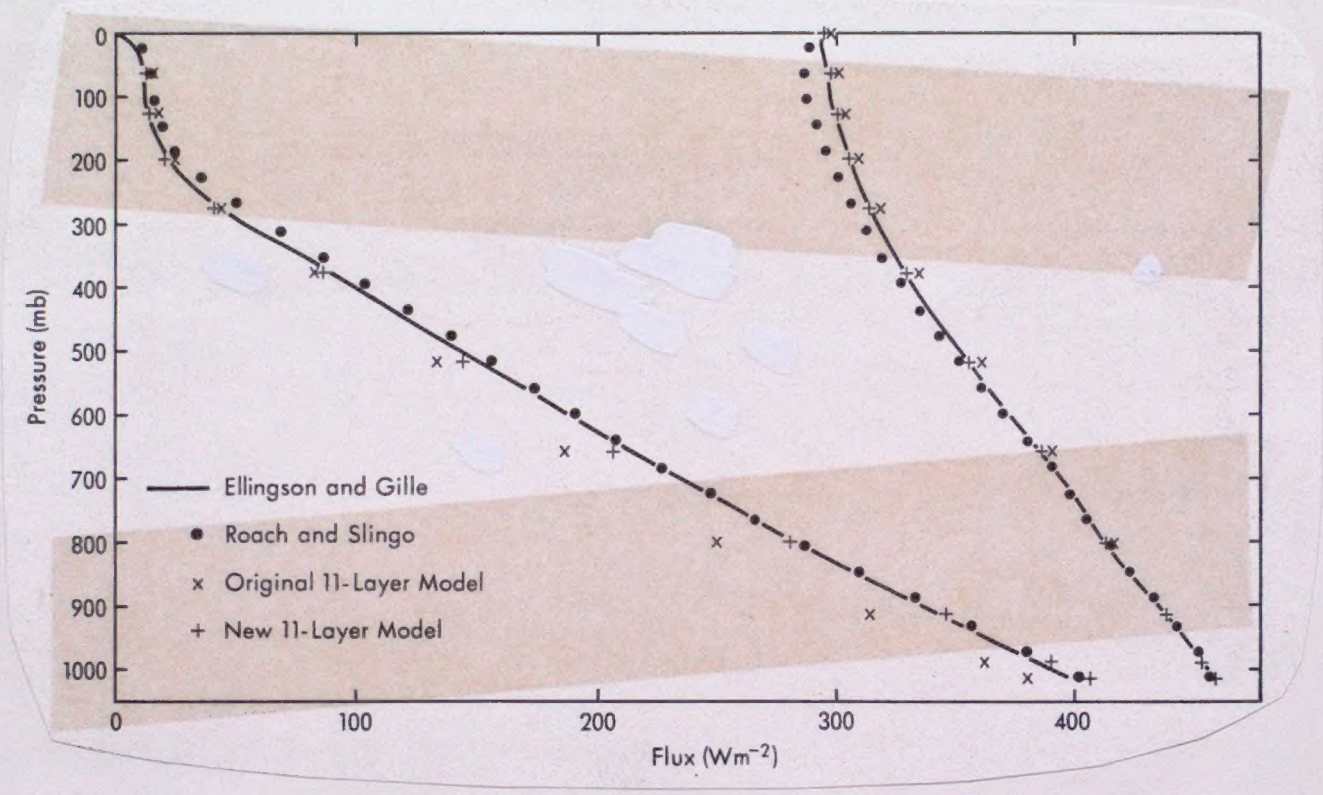

Figure 2 Comparison of longwave fluxes from the Ellingson and Gille (1978), Roach and Slingo (1979), and the original and new versions of the 11-Layer Model scheme, for the McClatchey et al (1971) Tropical atmosphere.

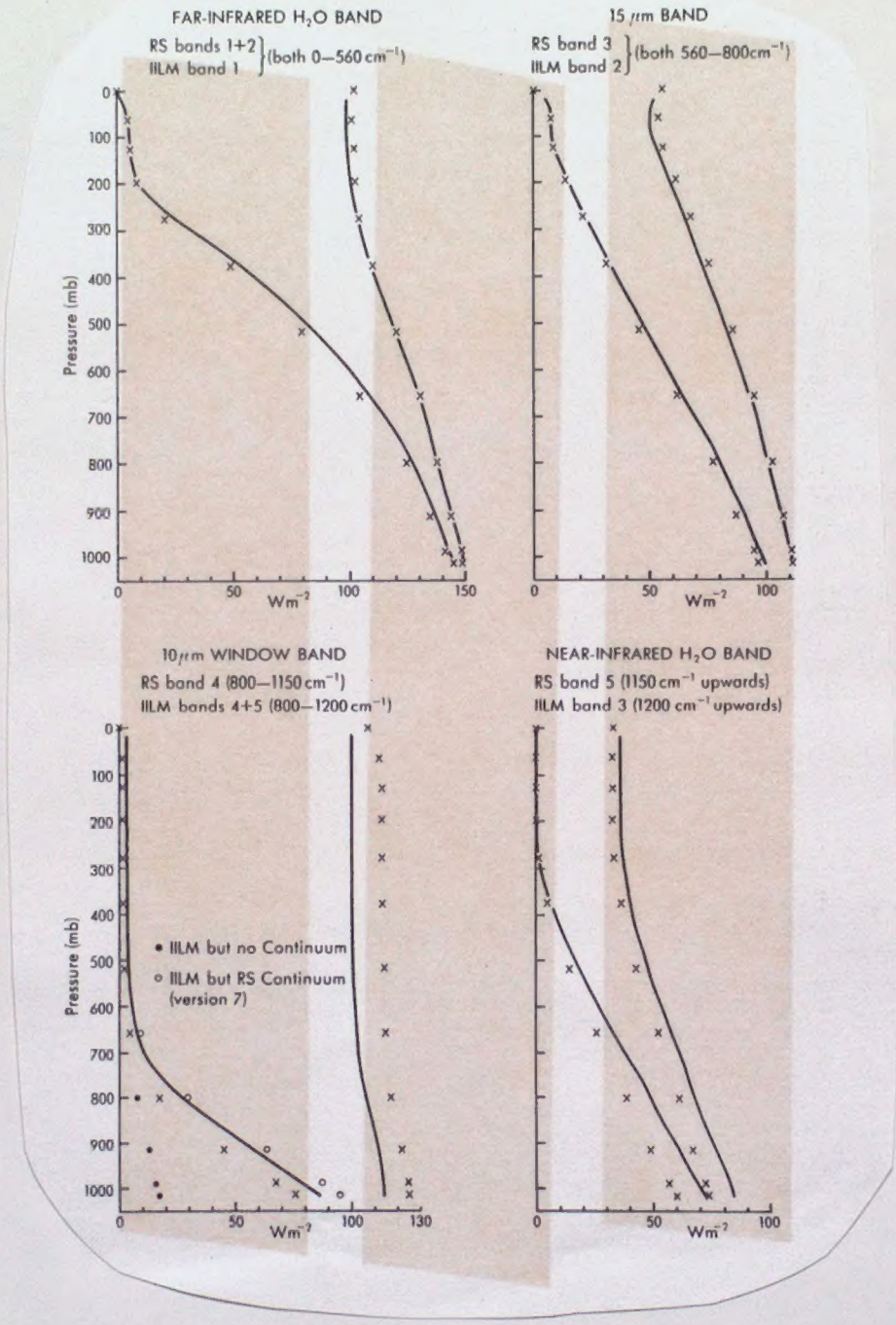

Figure 3 Comparison of longwave fluxes in selected spectral regions from the Roach and Slingo (1979) scheme (RS; shown as the solid lines) and Version 6 of the 11-Layer Model scheme (11LM; shown as the crosses), for the McClatchey et al (1971) Tropical atmosphere.

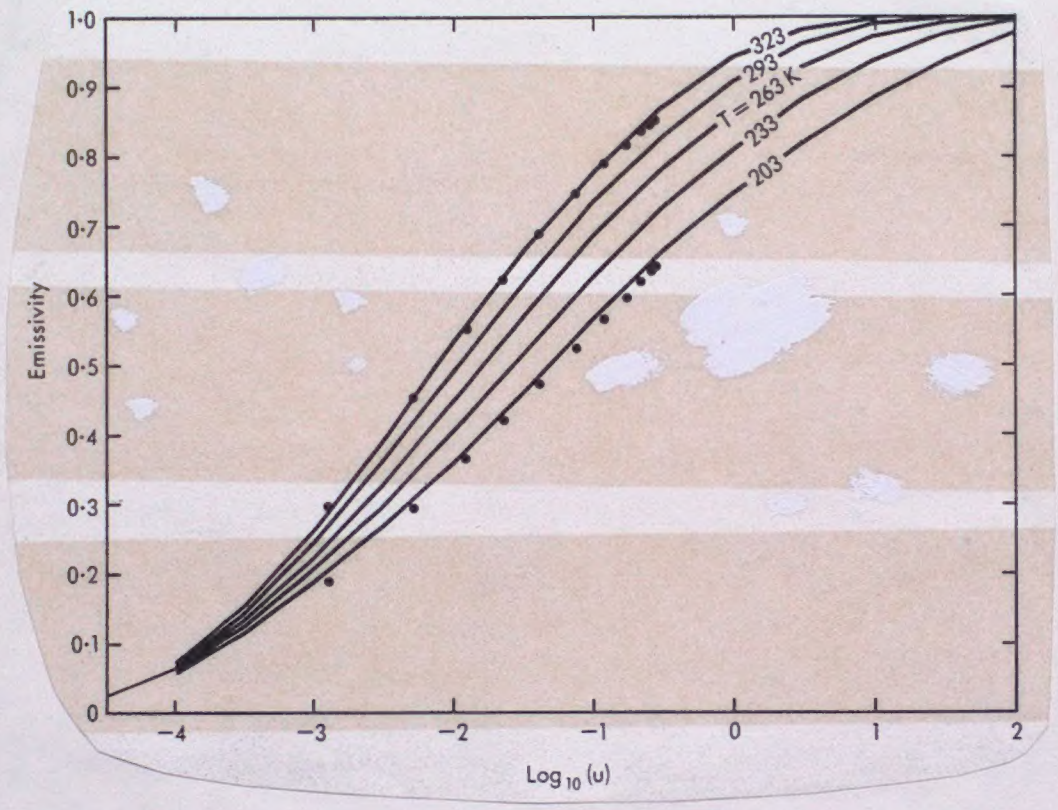

Figure 4 Normalized CO_2 emissivity for 560–800 cm^{-1} for various temperatures as a function of the absorber amount u (in g cm^{-2}). Emissivities at 203 K and 323 K obtained from the 263 K data by scaling the absorber amounts according to equations 8 and 9 are shown as the dots.